Preparation and characterisation of magnetosomes based drug conjugates for cancer therapy

Varalakshmi Raguraman[1], Krishnamurthy Suthindhiran[1] ✉

[1]*Marine Biotechnology and Bioproducts Laboratory, School of Biosciences and Technology, Vellore Institute of Technology, Vellore-632014, Tamilnadu, India*
✉ *E-mail: ksuthindhiran@vit.ac.in*

Abstract: The authors report a novel, effective and enhanced method of conjugating anticancer drug, paclitaxel and gallic acid with magnetosomes. Here, anticancer drugs were functionalised with magnetosomes membrane by direct and indirect (via crosslinkers: glutaraldehyde and 3-aminopropyltriethoxysilane) adsorption methods. The prepared magnetosome–drug conjugates were characterised by Fourier transform infrared, zeta potential, field-emission scanning electron microscope and thermogravimetric analysis/differential scanning calorimetry. The drug-loading efficiency and capacity were found to be 87.874% for paclitaxel (MP) and 71.3% for gallic acid (MG), respectively as calculated by ultraviolet spectroscopy and high-performance liquid chromatography. The drug release demonstrated by the diffusion method in phosphate buffer (PBS), showing a prolonged drug release for MP and MG, respectively. The cytotoxicity effect of the MP and MG displayed cytotoxicity of 69.71%, 55.194% against HeLa and MCF-7 cell lines, respectively. The reactive oxygen species, acridine orange and ethidium bromide and 4, 6-diamidino-2-phenylindole staining of the drug conjugates revealed the apoptotic effect of MP and MG. Further, the regulation of tumour suppressor protein, p53 was determined by western blotting which showed an upregulation of p53. Comparatively, the magnetosome–drug conjugates prepared by direct adsorption achieved the best effects on the drug-loading efficiency and the increased percentage of cancer cell mortality and the upregulation of P53. The proposed research ascertains that magnetosomes could be used as effective nanocarriers in cancer therapy.

1 Introduction

Nanoparticles are gaining huge attention in biomedical applications due to their superior physicochemical properties [1]. Numerous attempts have been made to improve the solubility and the effectiveness of anticancer drugs such as nanoformulations, liposomes, microspheres and parental emulsions [2]. The rationale behind this attempt is to improve the drug efficacy thereby reducing the side effects. The currently available chemotherapeutic drugs have the disadvantage of side effects, poor efficacy and lack of specificity towards cancer cells thereby affecting the other tissues and organs such as liver, kidney, heart etc. which in turn reduces the bioavailability of the drug to the target site and is responsible for extending the anticancer treatment in patients. Besides, the rapid drug clearance and the difficulty in drug permeability through the cells further contribute to the ineffectiveness of the existing treatment methods [3]. The repeated problems occurring in conventional chemotherapy methods to cure advanced cancer stages are in critical need of new approaches. Use of magnetic nanoparticles facilitates specific distribution and targeted delivery of loaded molecules thereby enhancing bioavailability, pharmacokinetic properties and therapeutic efficacy [4, 5]. Reports showed that functionalised magnetic nanoparticles encapsulated by a drug resulted in stable, biocompatible, less toxic, increased therapeutic effectiveness and prolonged survival rates in patients [6]. The method involves modifying the surface of nanoparticles with crosslinkers to couple or encapsulate the drug. The use of crosslinkers can induce side effects that can lead to toxicity that can also damage healthy cells or tissues nearby [7, 8]. Therefore, to evade these problems a biological nanoparticle can be utilised. Biogenic nanoparticle synthesised by magnetotactic bacteria called Bacterial magnetosomes, which have received a great interest in the biomedical field due to their unique properties: highly biomineralised inorganic crystal, organic magnetosome membrane, high surface to volume ratio, narrow size distribution and its low toxicity and biocompatibility [9]. Magnetosomes are iron oxide nanoparticles biomineralised by magnetotactic bacteria

which helps the bacteria for navigation with the response to the earth's magnetic field. The magnetosome membrane consists of phospholipids and proteins which are similar to the other cell membranes [10]. The biocompatibility of magnetosomes have been demonstrated by Sun *et al.* [11] 2009 in earlier studies showing slight toxicity in the organs of rats and also cytotoxicity against H22, HL60, EMT6 cells [12]. Hence magnetosomes exhibit excellent biocompatibility due to the membrane-bound structures. Owing to these properties, magnetosomes are promising candidates for a variety of biomedical and biotechnological applications, especially for cancer therapy [9, 13]. Here we chose two anticancer drugs: gallic acid (GA) and paclitaxel for the functionalisation of magnetosomes. These drugs are derived from natural sources, paclitaxel extracted from the bark of pacific yew (*Taxus brevifolia*) and GA from fruits, plants and food, respectively [4, 5, 14]. These drugs can induce apoptosis in cancer types like breast, liver etc. However, the clinical application of these drugs is hampered by its hydrophobic nature and the reported side effects like neurotoxicity, nephrotoxicity and hypersensitivity [7, 8].

In this study, we demonstrate the beneficial application of magnetosomes derived from magnetotactic bacteria, which were anaerobically cultivated. Further functionalised with anticancer drugs paclitaxel and GA by direct and indirect adsorption method. The resulting drug conjugated nanoparticles were characterised by Fourier transform infrared (FTIR) spectroscopy, ultraviolet (UV) spectroscopy, zeta potential, thermogravimetric analysis (TGA) and differential scanning calorimetry (DSC) and the P53 protein expression levels were measured by western blot. Hence the result explains the effective method of preparing magnetosome–drug conjugates by direct adsorption with the enhanced anticancer property.

2 Materials and methods

paclitaxel purchased from SRL Ltd (India), GA and glutaraldehyde solution (25%) was purchased from Himedia (India). 3-aminopropyltriethoxysilane (APTES) was purchased from Sigma-

Aldrich (India). All the reagents obtained commercially were of analytical grade and were used as received without further purification.

2.1 Preparation of magnetosome–drug conjugates

The culturing of MTB (MSR-1 strain) and extraction of magnetosomes and their characterisation were reported in our previous study [15]. The preparation and characterisation of magnetosome–drug conjugates were followed according to Raguraman and Suthindhiran 2019 [8, 15, 16]. Briefly, the magnetosomes (10 mg) resuspended in 10 ml phosphate buffer saline (PBS) (pH 7.4) were sonicated at 30 W for 1 h for complete dispersion. To this combination paclitaxol (1 mg/ml) dissolved in water (pH 1.2) and sonicated in a water bath sonicator for 2 h with 5 min pulse per 1 min and incubated overnight in an orbital shaker (60 rpm).

2.1.1 Determination of incorporated drug on magnetosomes:
To ensure the incorporated drugs: paclitaxel and GA, the magnetosome–drug conjugates were dispersed in methanol and vortexed vigorously and kept overnight [17]. The solution was centrifuged at 15,000 rpm for 30 min and the supernatant was obtained. The filtered supernatant was measured using high-performance liquid chromatography (HPLC). The standard solution of both paclitaxel and GA was prepared and used to prepare calibration curves ranging from 5 to 100 μg/ml. The drug content was calculated using the following equation:

$$\text{Drug content} = \text{Amount of drug in nanoparticles} / \text{Amount of nanoparticles} \times 100\%$$

2.1.2 Chromatography condition: *Paclitaxel*:
A HPLC system (Shimadzu) was used for the liquid chromatography system. The mobile phase consisted of acetonitrile (70:30 v/v). The separation was performed on a reverse phase C18 column and the column temperature was maintained at 30°C. The flow rate was set at 1 ml/min and the detection wavelength was 227 nm. The sample solution was injected at a volume of 20 μl.

Gallic acid: A HPLC system (Shimadzu) was used for the liquid chromatography system The mobile phase consisted of 0.1% phosphoric acid in methanol and 0.1% phosphoric acid acetonitrile (10:90 v/v). The reverse phase column was a C18 and the column temperature was maintained at 30°C. The flow rate was set at 1 ml/min and the detection wavelength was 270 nm. The sample solution was injected at a volume of 20 μl.

2.2 Characterisation of drug-loaded magnetosomes

Briefly, the lyophilised drug load magnetosomes were sonicated to disperse the magnetosome and a drop of this suspension was placed on the copper grids. After being dried, the grids were sputter coated and then observed under the Field emission scanning electron microscope (FE-SEM, Carl Zeiss, SUPRA 55VP, Germany). The surface charge of magnetosomes was analysed by zeta potential (HORIBA SZ-100, Japan).

2.3 Thermogravimetric analysis and differential scanning colorimetry

The drug (paclitaxel and GA) coated and uncoated magnetosomes were analysed by the thermogravimetric analyser and DSC, which helps to study the thermal behaviour of the sample [16]. TGA was analysed on NETZSCH STA 449 *F3*Jupiter®, at Central Electro Chemical Research Institute (CECRI), Karaikudi, Tamilnadu, with a heating rate of 10°C/min in air atmosphere from room temperature to 1000°C. DSC thermogram analysis of the samples was conducted using DSC, Model Q2000 (TA Instruments, USA). DSC cell was purged with 50 ml/min dry nitrogen. Accurately weighed samples (3–5 mg) were run in the standard aluminium pan in a temperature range of 25–300°C using a heating rate of 20°C/min and the melting point of the samples were determined from the thermogram [16].

2.4 In vitro drug release

The drug release from the magnetosome–drug conjugates was subjected to in vitro drug release study [18]. Paclitaxel coupled magnetosomes and GA-coupled magnetosomes (5 mg) were dispersed in 10 ml of PBS (pH 7.4) individually and incubated at 37°C under magnetic stirrer. At different time intervals, the supernatant was collected and analysed by UV spectroscopy.

2.5 Cell culture

The in vitro study was carried out on cervical cancer cell line (HeLa) and breast cancer cell line (MCF-7) cell line, confluent cells were passaged and maintained at 37°C in Dulbeccos modified Eagles medium (Gibco, Thermo Scientific) supplemented with 10% foetal bovine serum (Himedia) and antibiotic containing 50 U/ml penicillin, 50 mg/ml of streptomycin and actinomycin under a humidified atmosphere (5%, CO_2, Eppendorf).

2.5.1 Cytotoxicity assay:
HeLa and MCF-7 cells were grown in 96 well plates until confluent. Magnetosome-conjugated paclitaxel was added to the HeLa cells at different concentrations (100, 250, 500 and 1000 μg/ml) and incubated for 24 h. Similarly, magnetosome-conjugated GA was added to MCF-7 cells, after incubation, the media was discarded and the cells were washed with sterile PBS. After thorough washing, to each well 90 μl of fresh media and 10 μl of 3-(4,5-dimethylthiazol-2-yl)-2,5-diphenyltetrazolium bromide (MTT) (5 mg/ml stock) was added and incubated for 24 h in an incubator. The MTT was discarded from each well and 100 μl of DMSO was added to solubilise the formazan crystals formed. Absorbance was measured using a Microplate reader (LIMR96, Lark Innovative Fine Teknowledge, India) at 570 nm. The cell viability was calculated by the formulae

$$\text{Cell viability} (\%) = (\text{Absorbance of sample} / \text{Absorbance of control}) \times 100.$$

2.6 Apoptosis induced by magnetosome–drug conjugates

2.6.1 Acridine orange (AO)/ ethidium bromide (EB) staining for apoptosis:
The magnetosome–drug conjugates induced apoptosis was determined by AO/EB staining as described earlier [16]. Briefly, In a six-well title plate, cell lines of HeLa and MCF-7 were grown on coverslips, respectively, until they reached 80% confluence. The cells were treated with magnetosome conjugates of paclitaxel and GA (MP, MGP and MAG; MG, MGG and MAG) and incubated at 37°C for 24 h. After the incubation the cells were washed with PBS (pH 7.4, 0.01 M), fixed for 10 min with absolute methanol and washed again with PBS twice. The cells were stained for 10–15 min with 1 μl of AO/EB mixture (AO/EB 100 μg/ml) the cells were subsequently washed with PBS. The fixed cells were visualised under a fluorescent microscope (FM3000, WESWOX, India).

2.6.2 Intracellular reactive oxygen species (ROS) detection by fluorescence microscopy:
The intracellular ROS level was determined by 2′,7′-dichlorodihydrofluorescein diacetate (DCFDDA) method [19]. In brief Hela cells (2×10^4) were seeded on a coverslip in six-well titre plate until confluent. The cells were treated with drug conjugated magnetosomes of various concentrations and incubated at 37°C for 24 and 48 h. The cells were washed twice with cold 0.001 M PBS (pH 7.4) and 2′, 7′ -dichlorofluorescin diacetate (DCFDA) was added and incubated for 10 min at room temperature and the cells were viewed and imaged by fluorescent microscope (FM3000, WESWOX, India).

2.6.3 6-diamidino-2- phenylindole staining:
Apoptosis was identified morphologically by DAPI staining [19]. The HeLa cells (1×10^5) were seeded on a coverslip in a six-well titre plate and treated with paclitaxel, magnetosomes, magnetosome-coupled paclitaxel, respectively, cultured at 37°C for 24 h. Similarly, MCF-7 cells (1×10^5) were seeded on a coverslip in a six-well titre plate and treated with magnetosomes, GA and magnetosome-
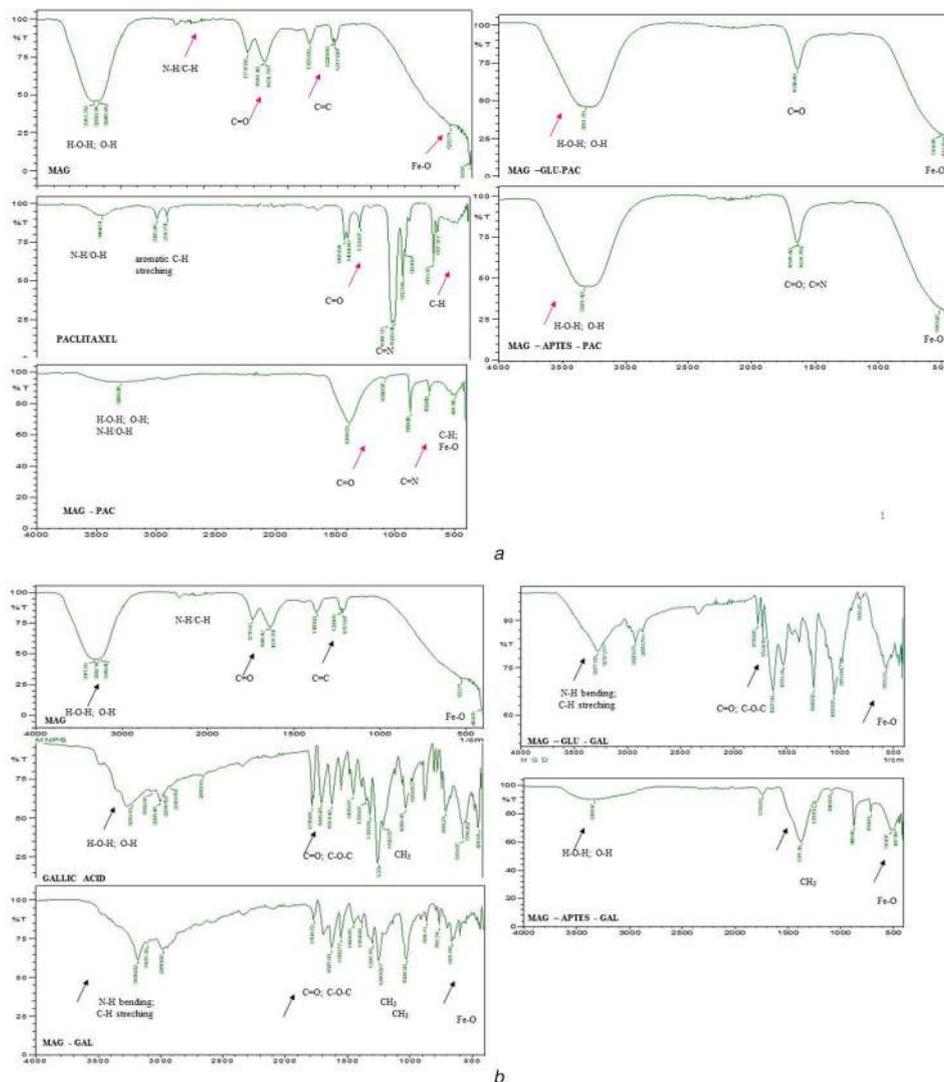
Fig. 1 *FTIR spectrum of*
(a) Magnetosome (MAG), paclitaxel, paclitaxel conjugated magnetosomes (MAG–PAC), paclitaxel conjugated magnetosomes via glutaraldehyde (MAG–GLU–PAC) and paclitaxel conjugated magnetosomes via APTES (MAG–APTES–PAC), *(b)* Magnetosome (MAG), GA, GA-conjugated magnetosomes (MAG–GAL), GA-conjugated magnetosomes via glutaraldehyde (MAG–GLU–GAL) and GA-conjugated magnetosomes via APTES (MAG–APTES–GAL)

coupled GA, respectively, cultured for 24 h at 37°C. The cells were then washed twice with 0.001 M, PBS (pH 7.4) and stained with DAPI in PBS at room temperature for 15 min and washed twice with PBS and water. The coverslips were mounted on a glass slide and viewed under a fluorescence microscope (FM 3000, Weswox, India).

2.7 SDS PAGE and western blots

After the treatment, cells were homogenised and protein concentration was determined by Bradford's method ([20] Kruger, 2009) from the cell lysate. For western blot, the proteins (40 µl) were separated by SDS-PAGE and transferred to a nitrocellulose membrane in a semi-dry blot (Himedia). The blots were immunoblotted with P53 specific primary antibody (1:10,000) overnight at 4°C with agitation, then with Horseradish peroxidase (HRP)-conjugated secondary antibody (1:5000) for 1 h at room temperature. The blots were reprobed for Beta-actin, which is internal control. Immunoreactive proteins were detected by ECL (Santacruz, CA, USA) western blotting detecting system, normalised by β-actin [21].

3 Results and discussion

3.1 Characterisation of functionalised magnetosomes

The FTIR analysis explains the characteristic chemical structure of magnetosomes, the free drug and the drug conjugated

magnetosomes (Figs. 1*a* and *b*). The conjugation of magnetosome and drug (paclitaxel and GA) were achieved through the bonding of amino or carboxyl groups of lipid membrane present around magnetosomes and the functional groups present in the drug. The FTIR spectra of bacterial magnetosomes showed the characteristic absorption peaks: 3311.70, 3269.34, 2040.41, 1737.86, 1641.42, 1631.78, 1365.60, 1228.66, 1217.08 and 522.71. The characteristic absorption bands near 3311–3270 cm^{-1} represent the O–H and H–O–H bonds while the peaks at 522 cm^{-1} assigned to stretching vibration for Fe–O bond [22]. The FTIR spectra of free drug (paclitaxel) showed characteristic peaks around 3454, 2995, 2912, 1435, 1408, 1308, 1041, 1020, 952, 929, 699 and 667. These peaks depict the vibrational band of paclitaxel, the characteristics peak around the region 3500 cm^{-1} is due to the N–H/O–H vibrations, 2900 cm^{-1} implies the aromatic C–H stretching vibrations of the compound, 1400–1310 cm^{-1} is due to the C=O stretching vibrations exhibited by the carbonyl groups of the compound, in the region 1200–1000: C–N stretching absorption of primary aliphatic amines, the aromatic band (C–H) deformation are found in the region <700 cm^{-1}. The peaks for MP are 3298.28, 1381.03, 1082.07, 869.90, 709.80 and 491.85 cm/1, MGP peaks are at 3311.78, 1639.49, 514.99 and 493.78 cm/1, MAP 3321.42, 1641.42, 1631.78 and 516.92 cm/1. In the FTIR spectra of MP, the peaks almost match with that of the peaks of magnetosomes and paclitaxel. Similarly, for GA, the FTIR spectrum is shown in Fig. 1*b*. The peaks for GA: OH stretch (3219.19, 3062.96, 2996.45,

2964.50, 2910.58 and 2650.19); C = O (1770.66, 1695.43, 1614.42, 1436.97, 1336.67, 1305.81 and 1240.23), C–O–C (1199.72, 1081.41 and 980.56) CH3 bend (898.23, 553.57, 534.28 and 435.91); MG: OH stretch (3180.62, 3105.39 and 2980.02); C = O stretch (1768.72, 1625.99, 1550.77, 1444.68 and 1384.89), C = C stretch (1296.16, 1246.02 and 1024); MGG: 3277.06, 3217.27, 2920.23, 2850.79, 1770.65, 1724.36, 1627.92, 1533.41, 1246.02, 1055.06, 979.84, 806.25 and 563.21; MAG: OH stretch (3331.07), 1739.79, 1371.39, 1230.58, 1083.99, 869.90, 709.80, 513.07 and 487.99. The shift of the bands at C = O and C = C was found greater in MG than MGP and MAP. Similar observations were explained in our previous findings [16]. Hence the results confirm that direct adsorption leads to maximum drug coupling than glutaraldehyde and APTES for both the cases. The maximum loading of the drug onto magnetosome may be due to the presence of functional groups on the magnetosome membrane and high surface to volume ratio.

3.2 Surface charge

The surface charge of magnetosome and paclitaxel conjugated magnetosomes are shown in Table 1. The table depicts the changes in the surface charge of drug conjugates in comparison with magnetosomes shows the functionalisation of a drug on to magnetosome surface. The previous report demonstrated the similar results explaining the surface charge and stability of nanoformulations carried with paclitaxel [8]. The zeta potential decreased to −10.3 from −17.4 mV for MP conjugates similarly for MG conjugates it decreased up to −11.4 mV. Thus it explains the negatively charged magnetosomes owing to an anionic carboxylate group on their surface. The positively charged nanoparticles result in enhanced internalisation and can interact easily with biological barriers. Guo *et al.* 2008 [23] reported the efficient use of glutaraldehyde as a coupling reagent and showed the highest capacity of drug loading. Our study confirms that direct adsorption method can be efficiently used in developing drug conjugates.

3.3 Loading efficiency and drug-loading capacity

The loading efficiency was determined by varying the drug concentration coupled with magnetosomes using crosslinker. The loading efficiency of magnetosome–paclitaxel conjugates are as follows 87.874% for MP, 76.823% for MGP and 79.753% for MAP for a drug concentration of 1 mg/ml. Similarly for the loading efficiency for magnetosome–GA conjugates are 71.3% for MG, 43.851% for MGG and 87.771% for MAG, respectively. It is observed that the high-loading efficiency was found for conjugates prepared by direct conjugation (MP and MG), this may be due the high surface area and the lipid bilayer surrounded on magnetosomes which enabled the maximum loading of the drug. The drug-loading capacity was also calculated for magnetosome–drug conjugates. The amount of drug obtained from the conjugates is 878.74, 768.23, 797.53 µg/ml for MP, MGP and MAP and 713.56, 438.51, 877.71 µg/ml for MG, MGG and MAG, respectively. The HPLC analysis was carried out to determine the presence paclitaxel in magnetosomes and to quantify the loaded drug onto magnetosome. The supernatant of each drug conjugates was subjected to HPLC analysis. The peak reveals the presence of drug conjugated to magnetosomes in comparison with the standard. The characteristic peak of paclitaxel and GA was observed at a retention time of 4.5 and 2.6 min, respectively. The supernatant of each drug conjugates analysed showed peaks similar to the standard. Thus, it implies the presence of the drug adsorbed to the surface of magnetosomes. The drug-loading efficiency was also determined by HPLC, the system was calibrated using the standard solution (10–100 µg/ml) of paclitaxel and GA, respectively, where the correlation coefficient of the standard was $R^2 = 0.966$. The results prove that the magnetosome membrane is capable of loading a maximum amount of drug than the crosslinkers. Similar studies were performed by Guo *et al.* 2010 [24] showing a drug loading, i.e. 9.2% for direct adsorption and better drug loading for drug conjugates prepared by a different crosslinker. Our study showed a better and enhanced drug loading for direct adsorption this may be due to the abundant functional groups present on the surface of the magnetosome membrane.

3.4 In Vitro drug release

The drug release study was performed to evaluate the release of drug at a particular time, stability and also to suppress the adverse reaction of the drug. To evaluate the potential of magnetosome as a drug carrier, drug release behaviour was analysed. From Fig. 2, a slow and consistent release was observed from MP than others (MGP and MAP). The drug release from direct adsorption (MP) was 4, 41.3 and 82.01% after 2, 24 and 48 h, respectively. Among the crosslinker, MGP showed slow drug release (40.88, 41.99 and 33.82%) than MAP (77.07, 69.26 and 34.76%). The MAP showed an initial outburst immediately after 2 h of incubation and kept decreasing as the time increases similarly for MGP. Similarly for GA-magnetosome conjugates. The drug release of GA-magnetosomes conjugates prepared by direct adsorption is 27.07, 39.266 and 34.766% after 2, 24 and 48 h, respectively. From the observation, the drug release from the direct adsorption showed slow release than the conjugates prepared via crosslinkers, thereby helping the drug to reach the target site. The previous report

Table 1 Zeta potential of magnetosome drug conjugates: paclitaxel and GA

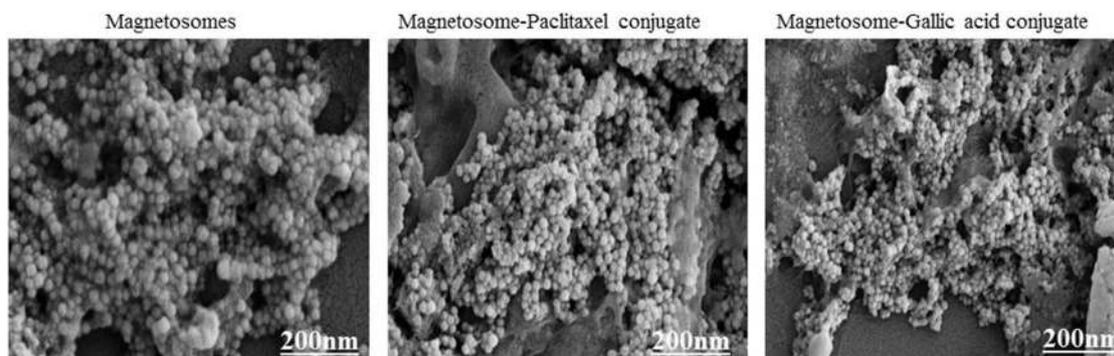| Magnetosome–paclitaxel drug conjugates		Magnetosome–GA drug conjugates	
Groups	Surface charge	Groups	Surface charge
MP	−10.3	MG	−11.4
MAP	−19.6	MAG	−24.4
MGP	−27.7	MGG	−31.3

Fig. 2 *Microscopic image of drug-coated and drug-uncoated magnetosomes observed under FE-SEM, magnification of 200 nm*
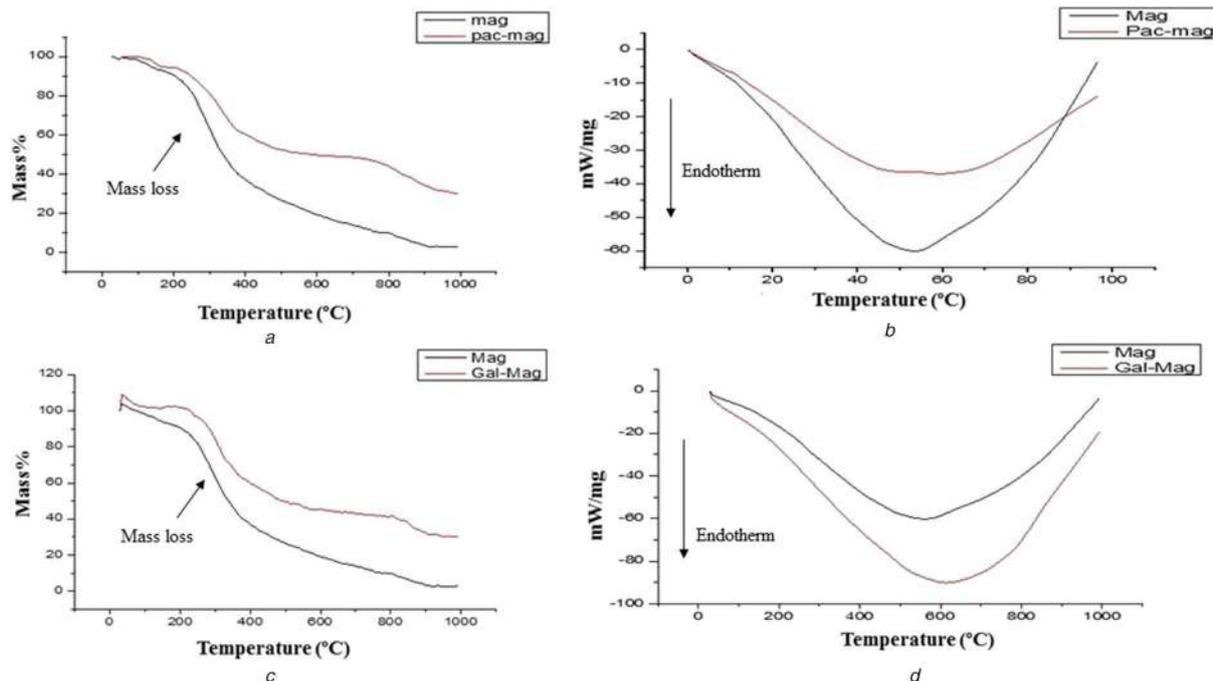*(a)* Uncoated magnetosomes, *(b)* Paclitaxel-coupled magnetosomes, *(c)* GA-coupled magnetosomes

Fig. 3 *TGA and DSC peaks of magnetosome–drug conjugates, showing the presence of drug coupled to the magnetosomes*
(a) TGA of paclitaxel-coupled magnetosomes, *(b)* DSC of paclitaxel-coupled magnetosomes, *(c)* TGA of GA-coupled magnetosomes, *(d)* DSC of GA-coupled magnetosomes
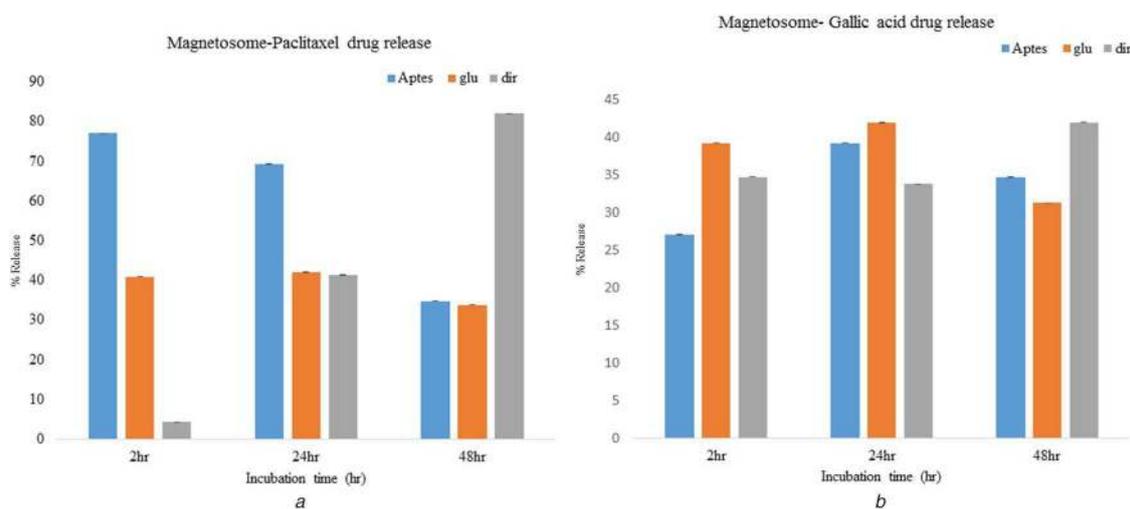

Fig. 4 *In vitro drug release studies of magnetosome–drug conjugates: dir (direct adsorption); indirect adsorption by crosslinker: glu (glutaraldehyde) (APTES)*

describes the release of aclitaxel from HGC nanoparticles loaded paclitaxel showed 50% drug release after 1 day and sustained 80% of drug release for 10 days [25]. Danhier et al. [26] 2007, demonstrated the initial drug release after 4 h was $46.9 \pm 5.7\%$ and the cumulative drug release was $75.3 \pm 2.7\%$., the initial outburst of paclitaxel may be due to the diffusion poorly entrapped drug within the polymer matrix.

3.5 Characterisation of drug-loaded magnetosome by FE-SEM

The morphology of paclitaxel- and GA-coated magnetosomes was observed by FE-SEM (Fig. 3). The magnetosomes have a cubo octahedral shape, therefore, they are observed in a spherical shape, they appear agglomerated due to the interaction with the drug and represent a porous network. The particle size of drug-coated magnetosomes is found larger than that of uncoated magnetosomes [27].

3.6 TGA/DSC of functionalised magnetosomes

The physical status of the native drug (paclitaxel and GA) coatings on the surface of magnetosomes were determined by TGA/DSC. TGA/DSC thermogram of magnetosomes with and without drug: paclitaxel and GA are represented in Fig. 4. DSC explains the characteristic melting endothermic peak, the change in the peak and the shift in the melting point suggests that the drug (paclitaxel and GA) is molecularly dispersed with magnetosomes showing amorphous nature that further infers the conformational change occurred with magnetosomes. Comparing the coated and uncoated magnetosomes, the difference in the thermal behaviour and physicochemical properties were observed, which depicts the possibility of conjugation. Hence, it confirms the coupling of the drug: paclitaxel and GA. Whereas the TGA graph explains the surface modification of drug: paclitaxel and GA adsorbed to the magnetosomes. To demonstrate the efficacy of drug: paclitaxel and GA coating on to magnetosomes with that of drug-free magnetosomes were taken for comparison. Fig. 4 shows the weight loss against the temperature of uncoated magnetosomes and paclitaxel-coated magnetosomes. The inset shows that magnetosomes degrade completely when heated up to 800°C
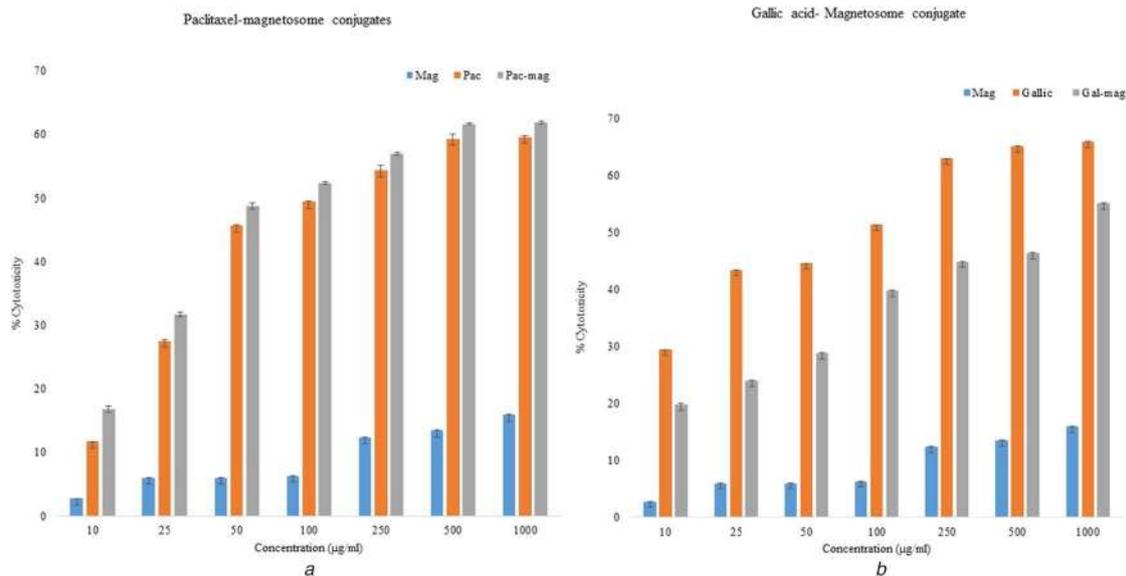
Fig. 5 *Cytotoxicity of magnetosome-based drug conjugates*
(a) Paclitaxel-conjugated magnetosome, *(b)* GA-conjugated magnetosome against HeLa and MCF7 cell lines, respectively
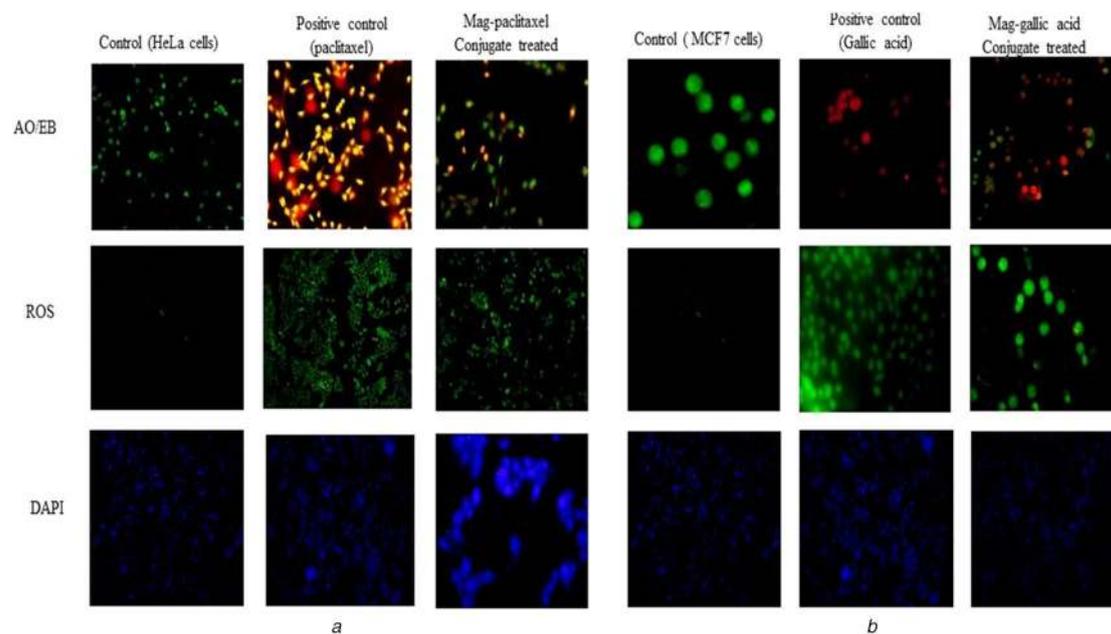

Fig. 6 *Apoptotic studies (AO/EB, ROS, DAPI) of magnetosome–drug conjugates*
(a) Magnetosome–paclitaxel conjugates, *(b)* Magnetosome–GA conjugates

(Fig. 3), and there is a distinct weight loss in the TGA curves of magnetosomes in which 60% weight loss was observed at 380°C. This loss of mass may be the decomposition and desorption of surface-bound proteins. Further mass loss explains a larger change occurred in the morphology of magnetosome by calcination. Whereas in paclitaxel loaded magnetosomes, the initial weight loss up to 100°C is due to desorption of physically adsorbed water. The weight loss from 200 to 500°C is due to the dehydration reaction of the coupled paclitaxel, a weight loss of 50% was observed at 400°C and it remained stable for up to 800°C and it dropped to 60% (weight loss) latter. Similar peaks were observed with slight changes for GA–magnetosomes conjugates [17].

3.7 Cytotoxicity assay

To assess the cytotoxicity of drug-loaded magnetosomes was determined against HeLa and MCF-7 cells by MTT assay. Among the prepared magnetosome–drug conjugates by direct adsorption, MP and MG were evaluated for cytotoxicity test, since the drug loading and efficiency were found high in MP and MG (direct adsorption) compared to conjugates prepared via crosslinkers

(MGP, MAP, MGG and MAG). The results of the MTT assay are shown in Fig. 5. The results were evident that the paclitaxel-loaded magnetosomes showed dose-dependent cytotoxicity against HeLa cells. Drug-free magnetosomes (only magnetosomes) did not cause significant change against the cell line, showing cell viability of 85%. However, the free drug showed cytotoxicity of 65.61% and 65.957% for paclitaxel and GA at a dose of 1 mg/ml, respectively, and 20.3% cell viability was observed. The effect of MP and MG against the cell lines did show significant cytotoxicity of 69.71% and 55.194% at a dose of 1 mg/ml similar to the standard drug paclitaxel and GA, respectively. The drug conjugated magnetosomes (MP and MG) could inhibit the cell viability similar to that of the free drug (paclitaxel and GA).

3.8 Apoptotic studies

3.8.1 AO/EB staining: The magnetosome–drug conjugates (MP and MG) treated on HeLa and MCF-7 cells (1×10^5), with the concentration of magnetosome–drug conjugate 1 mg/ml were subjected to AO/EB, ROS and DAPI staining (Fig. 6). In AO/EB staining, the control cells (viable cells) were stained green, while
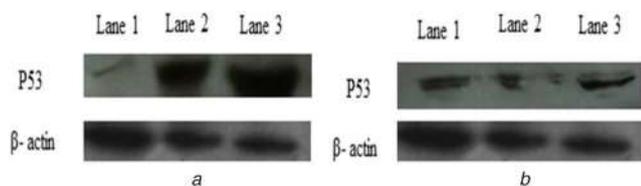
Fig. 7 *Western blot analysis of magnetosome–drug conjugates, showing the upregulation of p53 in treated cells in comparison with untreated cells*
(a) Western blot analysis of β-actin and p53 in cells treated for 24 h with Mag–PAC conjugate, magnetosome–paclitaxel conjugates treated on HeLa cells, *(b)* Western blot analysis of β-actin and p53 in cells treated for 24 h with Mag–GAL conjugate, magnetosome–GA conjugates on MCF-7. Lane 1, control; lane 2, positive control; lane 3, drug conjugates treated cells

treated cells stained orange, which depicts the apoptotic changes. Among the conjugates, MP-treated cells showed more green–orange stained cells compared to MGP and MAP. Similarly, GA magnetosome conjugate treated showed dead cells stained orange which depicts the apoptosis occurring. The pure drug: paclitaxel and GA, was served as positive control which was observed in red colour. The induced oxidative stress of functionalised magnetosomes was tested against the HeLa and MCF-7 cell lines by evaluating the intracellular ROS with $H_2DCFDDA$ assay (Fig. 6). In this study, when the HeLa cells were exposed to MP and MCF-7 were exposed to MG, there was a significant increase in the fluorescence intensity compared to control. The exposure of drug-loaded magnetosomes both MP and MG against HeLa and MCF-7 cells resulted in significant nuclear morphological changes observed after staining with DAPI under a fluorescent microscope (Fig. 6). The chromatin condensation was observed due to the stress, indicating the cytotoxicity effect. Thus the results suggest that MP- and MG-treated cells showed apoptotic changes than the other conjugates which depict that the maximum drug loaded than other conjugates. Baharara *et al.* 2016 [28] reported the apoptotic changes in HeLa cells treated with gold nanoparticles. Krishnaswamy *et al.* 2014 [19] reported the cytotoxicity and apoptotic effect of silver nanoparticles synthesised from *Indigofera aspalathoids*. Shukla *et al.* 2015 [29] demonstrated the cytotoxicity effect of chitosan oligosaccharide coated iron oxide nanoparticles. Further, to determine the effect of magnetosomes in anticancer therapy, we investigated the effects of chemotherapeutic agents (paclitaxel and GA) coupled with magnetosomes and analysed by Western Blot (Fig. 7). Here we compared the p53 expression in comparison with treated and untreated cells with magnetosome–drug conjugates. As known, p53 is a significant suppressor of tumours leading to apoptosis in the most DNA-damaging response agents mainly concerning the intrinsic pathway. The loss of the function p53 is observed in cancer cells, so when these cells are treated with anticancer drugs apoptosis occurs, therefore, the cell death also occurs. Our findings showed that both the magnetosome–drug conjugates increased apoptosis and thereby upregulating p53. β-actin was also monitored as an internal control. The expression of *p53* was found upregulated than the control or untreated cells.

4 Conclusion

The study describes the development of magnetosome-based drug conjugates to achieve an efficient nanocarrier for anticancer therapy by direct and indirect method (using crosslinker) of adsorption. Compared to the crosslinker, direct adsorption showed stronger coupling for MP and MG, respectively, with high-loading efficiency of 87.87 and 71.3%. The drug-loading capacity for MP and MG was also found to be 878.74 and 713.56 μg/ml, respectively, owing to a sustained, stable long-term drug release property with cytotoxicity of 65.71 and 55.194%. The obtained results showed that the methodology used in this study exhibited high drug integration efficiency (paclitaxel and GA). This also showed that the drug conjugated magnetosomes significantly improves the potency of anticancer as compared to free drug. Based on the results, the study reveals the importance of magnetosomes as a drug carrier in anticancer treatment thereby reducing the amount of drug and by improving the efficiency of treatment, therapy. The research provides a new approach to synthesising a magnetic-based drug nanocarrier. Henceforth, it can be concluded that the magnetosome–drug conjugates can be considered a promising in vivo drug-delivery system. However, further studies must be carried out in a clinical setting.

5 Acknowledgment

6 References

[1] Mohammed, L., Gomaa, H.G., Ragab, D., *et al.*: 'Magnetic nanoparticles for environmental and biomedical applications: A review', *Particuology*, 2017, **30**, pp. 1–14
[2] Surapaneni, M.S., Das, S.K., Das, N.G.: 'Designing paclitaxel drug delivery systems aimed at improved patient outcomes: current status and challenges', *ISRN Pharmacol.*, 2012, p. 623139
[3] Marques, J.G., Gaspar, V.M., Markl, D, *et al.*: 'Co-delivery of sildenafil (viagra®) and crizotinib for synergistic and improved anti-tumoral therapy', *Pharm. Res.*, 2014, **31**, (9), pp. 2516–2528
[4] Brigger, I., Dubernet, C., Couvreur, P.: 'Nanoparticles in cancer therapy and diagnosis', *Adv. Drug Delivery Rev.*, 2002, **54**, pp. 631–651
[5] Brannon-Peppas, L., Blanchette, J.O.: 'Nanoparticle and targeted systems for cancer therapy', *Adv. Drug Delivery Rev.*, 2012, **56**, pp. 1649–1659
[6] Parveen, S., Misra, R., Sahoo, S.K.: 'Nanoparticles: A boon to drug delivery, therapeutics, diagnostics and imaging', *Nanomed. Nanotechnol. Biol. Med.*, 2012, **8**, (2), pp. 73–124
[7] Yang, T., Choi, M.K., Cui, F.De, *et al.*: 'Preparation and evaluation of paclitaxel-loaded PEGylated immunoliposome', *J. Controlled Release*, 2007, **120**, pp. 169–177
[8] Zhang, Z., Feng, S.S.: 'Self-assembled nanoparticles of poly(lactide)-vitamin E TPGS copolymers for oral chemotherapy', *Int. J. Pharm.*, 2006, **324**, (2), pp. 191–198
[9] Alphandéry, E.: '*Applications of magnetosomes synthesized by magnetotactic bacteria in medicine*', vol. **2** (Frontiers Media S.A., USA, 2014)
[10] Gorby, Y.A., Beveridge, T.J., Blakemore, R.P.: 'Characterization of the bacterial magnetosome membrane', *J. Bacteriol.*, 1988, **170**, (2), pp. 834–841
[11] Sun, J.B., Wang, Z.L., Duan, J.H., *et al.*: 'Targeted distribution of bacterial magnetosomes isolated from magnetospirillum gryphiswaldense MSR-1 in healthy Sprague-Dawley rats', *J. Nanosci. Nanotechnol.*, 2009, **9**, (3), pp. 1881–1885
[12] Liu, R.T., Liu, J., Tong, J.Q., *et al.*: 'Heating effect and biocompatibility of bacterial magnetosomes as potential materials used in magnetic fluid hyperthermia', *Prog. Nat. Sci. Mater. Int.*, 2012, **22**, (1), pp. 31–39
[13] Vargas, G., Cypriano, J., Correa, T., *et al.*: 'Applications of magnetotactic bacteria, magnetosomes and magnetosome crystals in biotechnology and nanotechnology: mini-review', 2018
[14] Faried, A., Kurnia, D., Faried, L.S., *et al.*: 'Anticancer effects of gallic acid isolated from Indonesian herbal medicine, Phaleria macrocarpa (scheff.) boerl, on human cancer cell lines', *Int. J. Oncol.*, 2007, **30**, (3), pp. 605–613
[15] Raguraman, V., Suthindhiran, K.: 'Comparative ecotoxity assessment of magnetosomes and magnetite nanoparticles', *Int. J. Environ. Health Res.*, 2020, **30**, (1), pp. 1–13
[16] Zhang, Y., Ali, S.F., Dervishi, E., *et al.*: 'Cytotoxicity effects of graphene and single-wall carbon nanotubes in neural phaeochromocytoma-derived pc12 cells', *ACS Nano*, 2010, **4**, (6), pp. 3181–3186
[17] Soni, P., Kaur, J., Tikoo, K.: 'Dual drug-loaded paclitaxel–thymoquinone nanoparticles for effective breast cancer therapy', *J. Nanopart. Res.*, 2015, **17**, (1), p. 18
[18] Raguraman, V., Suthindhiran, K.: 'Comparative studies on functionalization of bacterial magnetic nanoparticles for drug delivery', *J. Cluster Sci.*, 2019, **31**, pp. 1–10
[19] Krishnasamy, L., Ponmurugan, P., Jayanthi, K., *et al.*: 'Cytotoxic, apoptotic efficacy of silver nanoparticles synthesized from *Indigofera aspalathoids*', *Int. J. Pharm. Pharm. Sci.*, 2014, **6**, pp. 245–248
[20] Kruger, N.J.: 'The bradford method for protein quantitation. The protein protocols handbook', 2009
[21] Jing, H., Wang, J., Yang, P., *et al.*: 'Magnetic fe3O4 nanoparticles and chemotherapy agents interact synergistically to induce apoptosis in lymphoma cells', *Int. J. Nanomedicine*, 2010, **5**, pp. 999–1004
[22] Revathy, T., Jayasri, M.A., Suthindhiran, K.: 'Toxicity assessment of magnetosomes in different models', *3. Biotech.*, 2017, **7**, (2), p. 126
[23] Guo, L., Huang, J., Zhang, X., *et al.*: 'Bacterial magnetic nanoparticles as drug carriers', *J. Mater. Chem.*, 2008, **18**, pp. 5993–5997
[24] Guo, L., Huang, J., Zheng, L.M.: 'Efficient conjugation doxorubicin to bacterial magnetic nanoparticles via a triplex hands coupling reagent', *J. Nanosci. Nanotechnol.*, 2010, **10**, (10), pp. 6514–6519
[25] Kim, J.H., Kim, Y.S., Kim, S., *et al.*: 'Hydrophobically modified glycol chitosan nanoparticles as carriers for paclitaxel', *J. Controlled Release*, 2006, **111**, (1–2), pp. 228–234
[26] Danhier, F., Lecouturier, N., Vroman, B., *et al.*: 'Paclitaxel-loaded PEGylated PLGA-based nanoparticles: in vitro and in vivo evaluation', *J. Controlled Release*, 2009, **133**, (1), pp. 11–17

[27] Sundar, S., Mariappan, R., Piraman, S.: 'Synthesis and characterization of amine modified magnetite nanoparticles as carriers of curcumin-anticancer drug', *Powder Technol.*, 2014, **266**, pp. 321–328

[28] Baharara, J., Ramezani, T., Divsalar, A.*, et al.*: 'Induction of apoptosis by green synthesized gold nanoparticles through activation of caspase-3 and 9 in human cervical cancer cells', *Avicenna J. Med. Biotechnol.*, 2016, **8**, (2), p. 75

[29] Shukla, S., Jadaun, A., Arora, V.*, et al.*: 'In vitro toxicity assessment of chitosan oligosaccharide coated iron oxide nanoparticles', *Toxicol. Reports*, 2015, **2**, pp. 27–39